Available online at www.elixirpublishers.com (Elixir International Journal)

Vibrational Spectroscopy

Elixir Vib. Spec. 91 (2016) 38039-38046

ISSN: 2229-712X

Vibrational spectra, NBO analysis and thermodynamic properties of N-(4-methoxybenzylidine) aniline by theoretical methods

F.Liakath Ali Khan[1], A.Md.Sabeelullah Roomy[1,*], G.Saravanan[1] and N.Nadeem Afroze[2]

[1]Department of Physics, Islamiah College (Autonomous), Vaniyambadi, India.

[2]Department of Chemistry, Islamiah College (Autonomus), Vaniyambadi, India.

ARTICLE INFO

Article history:

Received: 19 December 2015;

Received in revised form:

28 January 2016;

Accepted: 2 February 2016;

Keywords

N4MBA, DFT, HOMO, LUMO, NBO, TED.

ABSTRACT

The optimized molecular structure, vibrational frequencies, corresponding vibrational assignments and thermodynamic properties of N-(4-methoxybenzylidine) aniline (N4MBA) have been investigated by using *ab initio* HF/6-311++G(d,p) and DFT/B3LYP method at 6-311G(d,p) and 6-311++G(d,p) basis sets. The energy and oscillator strength calculated by TD-DFT are in line with experimental findings. Moreover, we have not only simulated HOMO and LUMO, but also determined the energy band gap. The stability of the molecule arising from hyperconjugative interaction and charge delocalization has been analyzed using natural NBO analysis. Besides, Mulliken charges were also calculated. IR and Raman intensities were calculated and TED also has been reported.

Introduction

The title compound N4MBA is a benzylidine aniline derivative. The derivatives of benzylidine aniline were extensively used in liquid crystals which has great scientific and technological importance. They are also used as corrosion inhibitors for zinc in hydrochloric acid [1]. Benzylidine aniline derivatives also exhibit second order nonlinear optical properties [2,3]. It is used for the synthesis of bioactive pyrimidine compounds [4] and also finds applications in the preparation of liquid-crystalline polymers [5]. The benzylidine derivatives are intermediates in various pharmaceuticals, agrochemicals and perfumes [6].

Balachandran et.al., [7] computed the NLO properties of biologically active molecule N-(p-methoxybenzylidine) aniline. The molecular geometry has been calculated. Akira Takase et.al., [8] studied the spectroscopic studies of the thermochromism of N-(2-hydroxy-4-methoxybenzylidine)-4-nitroaniline. J.W.Lewis et.al., [9] reported the infrared spectra of thin polysrystalline films of N-Benzylidineaniline. Helmi Neuvonen et.al., [10] observed the electronic character of the C-N bridging group in substituted benzylidine anilines by comparing the ^{13}C NMR chemical shifts with the experimental value. Literature survey reveals that to the best of our knowledge, *ab initio* HF, DFT calculations and experimental studies on N4MBA molecule have not been reported so far. Therefore, The present work deals with FT-IR and FT-Raman spectroscopic investigation of N4MBA utilizing HF/6-311++G(d,p) and DFT method with 6-311G(d,p)/6-311G++(d,p) as basis sets. The redistribution of ED in various bonding and anti-bonding orbitals and E2 energies have been calculated by NBO analysis using DFT method to give clear evidence of stabilization originating from the hyper conjugation of various intra-molecular interactions. The HOMO and LUMO analysis have been used to elucidate information regarding charge transfer within the molecule.

Tele:

E-mail addresses: sabeelphy@gmail.com

Experimental Details

The compound N4MBA in the solid form was purchased from Sigma-Aldrich Chemical Company (USA) with a stated purity of greater than 98% and was used as such without further purification.

The FT-Raman spectrum of N4MBA was recorded using the 1064 nm line of a Nd:YAG laser as excitation wavelength in the region 10-3500 cm^{-1} on a Brucker model IFS 66V spectrophotometer equipped with an FRA 106 FT-Raman module accessory. The FT-IR spectrum of this compound was recorded in the region 400-4000 cm^{-1} on an IFS 66V spectrophotometer using the KBr pellet technique. The spectrum was recorded at room temperature, with a scanning speed of 10 cm^{-1} per minute and at the spectral resolution of 2.0 cm^{-1}.

Computational Details

For meeting the requirements of both accuracy and computing economy, theoretical methods and basis sets should be considered. DFT has proved to be extremely useful in treating electronic structure of molecules. The density functional three parameter hybrid model (DFT/B3LYP) at 6-311G(d,p) / 6-311++G(d,p) basis sets level along with HF method was adopted to calculate the properties of the molecule in this work. All the calculations were performed using the Gaussian 03W program package [11] with the default convergence criteria without any constraint on the geometry [12].

Results and Discussion

Molecular Geometry

The optimized molecular structure of N4MBA is shown in Fig. 1. Optimized bond lengths, bond angles and dihedral angles of the molecule are predicted using HF/6-311++G(d,p) and B3LYP/6-311G(d,p)/6-311++G(d,p) levels are given in Table 1. The bond distance of C1-C2 is 1.40Å and 1.39Å at B3LYP/6-311++G(d,p) and HF/6-311++G(d,p) methods respectively.

Table 1. Geometrical parameters optimized in N4MBA [bond length (A°), bond angle (◦) and dihedral angle (◦)]

Parameters	HF/6-311G++(d,p)	B3LYP/6-311G(d,p)	B3LYP/6-311G++(d,p)
Bond length (Å)			
C1-C2	1.39	1.40	1.40
C2-C3	1.37	1.37	1.38
C3-C4	1.39	1.39	1.39
C 4-C5	1.38	1.40	1.40
C5-C6	1.38	1.38	1.38
C6-C1	1.38	1.39	1.39
C1-O11	1.34	1.39	1.39
O11-C12	1.40	1.43	1.43
C12-H13	1.08	1.09	1.09
C12-H14	1.08	1.09	1.09
C12-H15	1.08	1.09	1.09
C4-C28	1.48	1.52	1.52
C28-H29	1.08	1.08	1.08
C28-N16	1.25	1.35	1.35
N16-C17	1.40	1.44	1.44
C17-C18	1.39	1.39	1.39
C18-C20	1.38	1.39	1.39
C20-C24	1.38	1.39	1.39
C24-C22	1.38	1.39	1.39
C22-C19	1.38	1.39	1.39
C19-C17	1.39	1.39	1.39
Bond Angle (°)			
C1-C2-C3	119.7	120.4	120.4
C2-C3-C4	121.8	121.1	121.1
C3-C4-C5	117.5	117.6	117.6
C4-C5-C6	121.3	121.9	121.9
C5-C6-C1	120.0	119.5	119.5
C6-C1-C2	119.4	119.1	119.1
C1-O11-C12	120.2	114.8	114.8
O11-C12-H13	111.2	112.3	112.3
O11-C12-H14	106.1	106.3	106.3
O11-C12-H15	111.3	112.3	112.3
C4-C28-N16	112.8	109.6	109.6
C28-N16-C17	124.9	123.6	123.6
C18-C17-C19	119.2	119.9	119.9
C17-C19-C22	120.1	119.6	119.6
C19-C22-C24	120.6	120.5	120.5
C22-C24-C20	119.1	119.6	119.6
C24-C20-C18	120.5	120.2	120.2
C20-C18-C17	120.1	119.8	119.8
C18-C17-C19	119.2	119.9	119.9
C17-C19-C22	120.1	119.6	119.6
C19-C22-C24	120.6	120.5	120.5
C22-C24-C20	119.1	119.6	119.6
Dihedral Angle (°)			
C1-C2-C3-C4	-1.07	-1.06	-1.06
C2-C3-C4-C5	1.41	0.52	0.52
C3-C4-C5-C6	-0.60	-0.66	-0.66
C4-C5-C6-C1	-0.42	-0.41	-0.41
C5-C6-C1-C2	0.77	0.98	0.98
C6-C1-C2-C3	-0.04	-0.01	-0.01
C1-O11-C12-H13	61.0	61.0	61.0
C1-O11-C12-H14	179.8	179.5	179.5
C1-O11-C12-H15	-61.4	-61.8	-61.8
C4-C28-N16-C17	-2.97	-2.99	-2.99

The reasoning of larger bond length that appears in the bond is repulsive and attractive forces of unlike charges. The maximum bond length has been calculated for C4-C28 (1.52Å), N16-C17 (1.44Å) and O11-C12 (1.43 Å) by B3LYP/6-311++G(d,p). Optimized bond angles of C6-C1-C2 are 119.1° and 119.4° using B3LYP/6-311++G(d,p) and HF/6-311++G(d,p) methods respectively. The C1-O11-C12, O11-C12-H15 bonds have different angles (114.8° and 112.3°), the C-C-H bond angle of the molecule increases and decreases towards 120 degree. Among the bond angles of O-C-H, the O11-C12-H14 has minimum angle about

106.3°. The C-C-C bond angles have bond angle in the molecule (C18-C17-C19:

119.9°, C17-C19-C22: 119.6°, C19-C22-C24: 120.5° and C24-C20-C18: 120.2°). The planarity of the molecule is confirmed through the dihedral angle from 0° to 180°. In the absence of experimental values the theoretically calculated bond lengths, bond angles and dihedral angles are mutually correlate with each other.

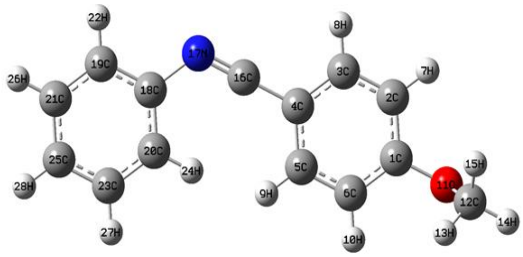

Figure 1. Optimized structure of N4MBA using B3LYP/6-311++G(d,p)

Vibrational Spectral Analysis

Vibrational spectral assignments were performed on the recorded FT-IR and FT-Raman spectra based on the theoretically predicted wavenumbers by *ab initio* HF/6-311++G(d,p) and DFT (B3LYP/6-311G(d,p)/6-311++G(d,p)) methods and are collected in Tables 2. The theoretically predicted IR and Raman spectra at B3LYP/6-311++G(d,p) level of calculations were shown in Figs. 2 and 3 respectively along with the experimental spectrum. None of the predicted vibrational spectra has any imaginary wavenumbers, implying that the optimized geometry is located at the local lowest point on the PES. We know that *ab initio* HF and DFT potentials systematically overestimate the vibrational wavenumbers. These discrepancies are corrected either by computing anharmonic corrections explicitly or by introducing a scaled field [13] or by directly scaling the calculated wavenumbers with proper scale factors [14, 15]. There are 81 normal modes of fundamental vibrations.

C-H Vibrations

In the heteroaromatic compounds, the C-H stretching vibrations normally occur at 3100-3000 cm^{-1}. These vibrations are not found to be affected by the nature and position of the substituent and typically exhibit weak bands compared with the aliphatic stretching vibrations. In IR spectra, most of the aromatic compounds have nearly four peaks in the region 3080-3010 cm^{-1} due to ring C-H stretching bands. IR frequencies of C-H bands are a function of sp hybridization [16]. The scaled vibrations, [mode nos: 69-80] assigned to the aromatic C-H stretch computed in the range 3168-3366 cm^{-1} by HF/6-311++G(d,p) method shows good agreement with the recorded weak FT-IR band. As expected, these fourteen modes are pure stretching modes as it is evident from TED column that they are almost contributing to 98%.

O-CH_3 Vibrations

In N4MBA, there is a O-CH_3 group attached to the benzene ring and we expect number of stretching and bending vibrations. In aromatic molecules, the asymmetric stretching vibrations of O- CH_3 are expected to appear in the range of 1705-1680 cm^{-1} [17]. In this study the harmonic frequencies 1699, 1750 and 1781 cm^{-1} (mode nos: 58, 59 and 60) by B3LYP/6-311++G(d,p) method are assigned to CH_3 symmetric stretching modes.

Ring Vibrations

The ring carbon-carbon stretching vibrations occur in the region 1625-1430 cm^{-1}. In general, the bands are of variable intensity and are observed at 1625-1575, 1540-1470, 1465-1430 and 1380-1280 cm^{-1} from the wavenumber ranges given by Shimanouchi et al., [18] for five bands in the region. In the present investigation, the wavenumbers observed at 1572 cm^{-1} in FT-Raman and 1577 cm^{-1} in FT-IR have been assigned to C=C stretching vibration. The theoretically computed values by B3LYP/6-311++G(d,p) at 1542, 1545, 1667, 1669 cm^{-1} [mode nos: 55, 56, 57, 58] show good agreement with experimental values. The aromatic stretching υ(c-c) vibrations give rise characteristic bands in both the observed IR and Raman spectra, covering the spectral range from 1600-1400 cm^{-1} [19-23].

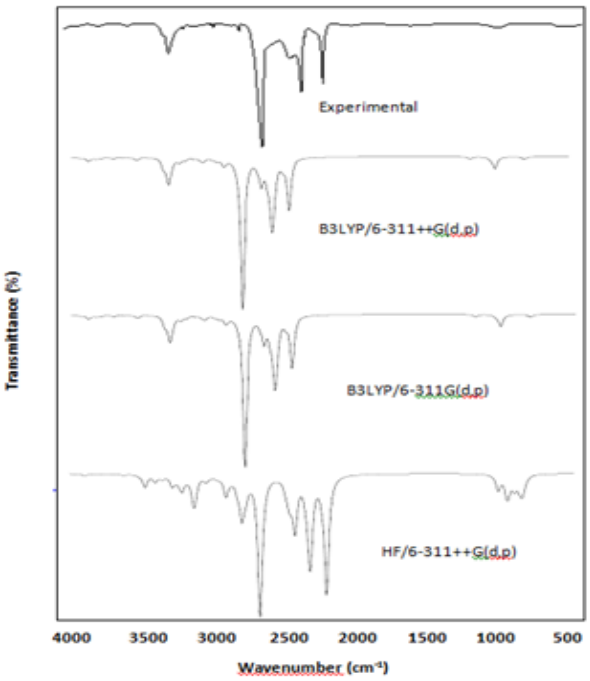

Figure 2. Comparison of the observed and computed

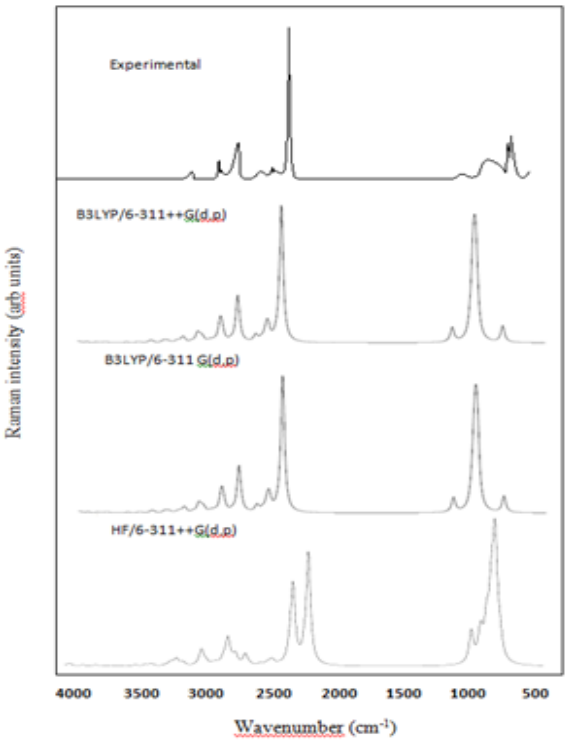

Figure 3. Comparison of the observed and computed FT- Raman spectra of N4MBA

Table 2. The observed FT-IR, FT-Raman and computed frequencies (cm^{-1}), IR, Raman intensities (Km/mol), reduced mass (amu) and force constants (mdyn/Å) of by using B3LYP/6-311G++(d,p)

Mode No.	Observed Freq. (cm^{-1})		Computed at B3LYP/6-311++G(d,p)					TED (%)
	FT-IR	FT-Raman	Freq. scaled	Intensity IR	Intensity Raman	Red. Mass	Force Const.	
υ_1			32	0.87	4.44	3.58	0.00	δ_{CCC} (45%)
υ_2			42	0.44	1.32	4.64	0.00	t_{CCNC} (59%) + t_{CCCN} (33%)
υ_3			63	0.18	1.64	4.71	0.01	t_{CNCC} (41%) + Γ_{CCCC} (24%)
υ_4			83	2.37	0.57	3.76	0.01	δ_{CCN} (12%) + δ_{CNC} (26%) + δ_{CCC} (12%)
υ_5			121	3.90	3.96	4.70	0.04	t_{CCOC} (63%)
υ_6			176	13.37	0.11	4.73	0.08	t_{CCNC} (19%) + t_{CCCN} (44%)
υ_7			208	4.37	2.77	4.93	0.12	t_{CCCC} (25%) + t_{CCCC} (25%)
υ_8			245	5.36	0.57	3.80	0.13	δ_{CCO} (29%) + δ_{CCC} (16%) + δ_{COC} (14%)
υ_9			279	5.22	1.70	1.27	0.05	t_{HCOC} (75%)
υ_{10}			305	2.40	2.29	2.96	0.16	δ_{CCC} (12%) + δ_{COC} (17%) + t_{CCCC} (12%)
υ_{11}			361	1.62	0.87	4.42	0.34	δ_{CCN} (11%) + δ_{CCC} (14%) + t_{HCOC} (10%)
υ_{12}			403	6.80	0.80	5.32	0.50	t_{CCCC} (10%) + t_{CCCN} (13%) + Γ_{CCCC} (25%)
υ_{13}			480	0.01	0.01	3.07	0.41	γ_{NC} (14) + δ_{CCO} (15%)
υ_{14}			483	2.84	0.42	3.22	0.44	t_{CCCC} (47%) + t_{CCCC} (32%)
υ_{15}	553w	508w	491	0.05	2.47	5.14	0.73	t_{CCCC} (66%) + t_{CCCC} (11%) + t_{CCCC} (12%)
υ_{16}			541	2.13	0.50	5.17	0.89	δ_{CCO} (12%) + δ_{COC} (29%)
υ_{17}			593	2.10	1.63	3.48	0.72	δ_{CCN} (18%) + δ_{NCC} (10%) + δ_{CNC} (13%)
υ_{18}			605	8.78	1.49	4.24	0.91	t_{CCCC} (10%) + Γ_{NCCC} (44%)
υ_{19}			618	1.41	0.89	3.03	0.68	Γ_{OCCC} (38%) + Γ_{CCCC} (13%)
υ_{20}		656w	705	0.88	1.31	5.59	1.63	γ_{CC} (17%) + δ_{NCC} (15%)
υ_{21}			712	0.28	3.99	6.35	1.89	δ_{CCC} (20%) + δ_{CCC} (10%) + δ_{CCC} (41%)
υ_{22}	767w		732	1.10	5.08	6.67	2.10	δ_{CCC} (33%) + δ_{CCC} (40%)
υ_{23}	788w		830	0.84	1.63	2.10	0.85	t_{CCCC} (55%) + t_{CCCC} (23%) + t_{CCCC} (18%)
υ_{24}			840	29.06	5.77	2.38	0.99	t_{HNCC} (31%) + t_{CCCC} (11%) + t_{CCCC} (17%)
υ_{25}			866	13.20	4.94	3.73	1.64	γ_{OC} (13%) + t_{HNCC} (17%)
υ_{26}			886	75.95	3.42	2.06	0.95	t_{HNCC} (42%) + t_{CCCC} (10%) + t_{CCCC} (10%)
υ_{27}			908	19.54	0.34	1.66	0.80	γ_{OC} (18%) + Γ_{CCCH} (11%)
υ_{28}			995	1.68	4.11	4.84	2.60	γ_{OC} (10%) + Γ_{CCCH} (11%) + Γ_{CCCH} (17%)
υ_{29}			978	15.05	5.09	1.96	1.10	t_{HCCO} (15%) + t_{HCCO} (24%)
υ_{30}	954w		1010	0.31	6.94	1.39	0.83	γ_{CC} (12%) + δ_{CCC} (12%)
υ_{31}			1025	4.08	5.97	1.57	0.97	t_{HCCO} (37%) + t_{HCCO} (45%)
υ_{32}			1026	5.79	8.48	1.76	1.09	Γ_{CCCH} (43%) + Γ_{CCCH} (45%)
υ_{33}			1104	4.30	4.30	1.36	0.97	γ_{CC} (16%) + δ_{NCC} (11%) + δ_{CNC} (23%)
υ_{34}			1154	1.55	21.27	5.43	4.26	Γ_{CCCH}(20%)+t_{HCCH} (12%)+t_{HCCH} (32%) + t_{HCCH}(27%)
υ_{35}		1064w	1156	1.26	5.24	1.36	1.07	γ_{CC} (18%) + γ_{CC} (10%) + δ_{CCC} (24%) + δ_{CCC} (13%) + δ_{CCC} (19%)
υ_{36}			1170	0.39	2.49	2.99	2.41	t_{HCCH} (28%) + t_{HCCH} (53%)
υ_{37}			1173	4.93	7.09	6.00	4.87	γ_{CC} (17%) + γ_{CC} (16%) + δ_{CCC} (19%) + δ_{CCC} (19%)
υ_{38}	1085w		1185	0.29	2.55	1.45	1.20	γ_{CC} (12%) + γ_{CC} (14%) + γ_{CC} (21%) + γ_{CC} (26%)
υ_{39}			1187	0.07	0.16	1.33	1.10	t_{HCCH} (57%) + t_{HCCH} (28%)
υ_{40}			1190	11.11	6.98	3.79	3.16	t_{HCCH} (47%) + t_{HCCH} (41%)
υ_{41}			1204	0.46	3.91	1.45	1.23	γ_{CC} (15%) + γ_{CC} (11%) + γ_{CC} (13%) + γ_{CC} (12%)
υ_{42}			1205	0.51	6.64	1.69	1.44	Γ_{CCCH} (11%) + t_{HCCH} (22%) + t_{HCCH} (58%)
υ_{43}			1265	2.30	4.53	1.50	1.42	γ_{CC} (10%) + γ_{CC} (14%) + γ_{CC} (21%)
υ_{44}			1280	3.31	3.48	3.47	3.35	γ_{CC} (14%) + δ_{HCC} (12%) + δ_{HCC} (20%) + δ_{HCC} (15%)
υ_{45}			1308	4.05	3.74	1.25	1.26	δ_{HCC} (17%) + δ_{HCC} (14%) + δ_{HCC} (13%) + δ_{HCC} (12%) + δ_{HCC} (12%)

Table 2 Continued….

Mode No.	Observed Freq. (cm^{-1})		Computed at B3LYP/6-311++G(d,p)					TED (%)
	FT-IR	FT-Raman	Freq. scaled	Intensity IR	Intensity Raman	Red. Mass	Force Const.	
υ_{46}			1309	5.10	0.51	1.42	1.44	Γ_{CHOH} (85%)
υ_{47}			1357	0.62	7.90	1.14	1.24	δ_{HCC} (13%) + δ_{HCC} (23%) + δ_{HCC} (26%)
υ_{48}			1367	20.17	54.44	1.35	1.49	δ_{HCC} (18%) + δ_{HCC} (22%)
υ_{49}			1372	3.11	2.72	1.18	1.32	δ_{HCC} (25%) + δ_{HCC} (24%)
υ_{50}			1382	1.29	25.38	1.97	2.21	γ_{CC} (14%) + δ_{HCO} (18%)
υ_{51}			1389	2.83	9.68	1.53	1.74	δ_{HCC} (18%) + δ_{HCO} (36%)
υ_{52}		1523ms	1468	5.39	5.43	2.98	3.79	γ_{OC} (15%) + γ_{NC} (10%) + γ_{OC} (53%)
υ_{53}			1528	272.6	85.97	1.89	2.60	γ_{NC} (24%)
υ_{54}	1540w		1532	192.4	57.86	1.86	2.57	γ_{NC} (32%) + δ_{HNC} (14%) + δ_{HCC} (17%)
υ_{55}	1543w		1541	40.00	12.84	1.51	3.25	γ_{NC} (21%) + δ_{HCC} (10%) + δ_{HCC} (10%) + δ_{HCC} (11%)
υ_{56}	1562w		1545	52.11	3.33	3.10	2.25	δ_{HCC} (12%) + δ_{HCC} (15%)
υ_{57}	1577s		1667	18.24	0.41	2.93	3.74	γ_{CC} (17%) + γ_{CC} (24%) + δ_{HCC} (13%)
υ_{58}			1699	76.57	22.53	1.91	3.25	δ_{HNC} (29%) + δ_{HCC} (15%) + δ_{HCC} (16%)
υ_{59}			1750	51.31	7.03	1.25	2.25	Γ_{CHHH} (74%)
υ_{60}			1781	70.66	10.17	2.00	3.74	δ_{HNC} (12%) + δ_{HCC} (10%) + δ_{HCC} (10%)
υ_{61}		2104ms	1795	168.2	13.73	2.66	5.06	δ_{HNC} (24%)
υ_{62}		2265ms	1806	2.78	28.65	1.05	2.02	δ_{HCC} (10%)
υ_{63}		2594vs	1812	43.07	9.06	2.34	4.54	δ_{HCH} (85%) + Γ_{CHOH} (12%)
υ_{64}			1817	0.92	21.12	1.13	2.20	δ_{HCH} (90%)
υ_{65}			1884	20.98	7.15	6.33	13.24	γ_{CC} (25%) + γ_{CC} (18%) + γ_{CC} (15%) + γ_{CC} (15%)
υ_{66}			1929	16.41	21.02	5.50	12.07	γ_{CC} (28%) + γ_{CC} (22%) + γ_{CC} (12%)
υ_{67}	2534w		1939	161.2	428.85	5.90	13.09	γ_{CC} (25%) + γ_{CC} (24%) + δ_{CCC} (10%)
υ_{68}	2679w		1944	2.50	8.75	6.01	13.38	γ_{CC} (36%) + δ_{CCC} (16%) + γ_{CC} (11%)
υ_{69}	2893ms		3528	7.28	47.46	1.03	7.60	γ_{CH} (37%) + γ_{CH} (25%) + γ_{CH} (38%)
υ_{70}			3697	4.25	24.26	1.10	8.92	γ_{CH} (50%) + γ_{CH} (49%)
υ_{71}	3123w		3710	0.39	8.51	1.08	8.83	γ_{CH} (11%) + γ_{CH} (47%) + γ_{CH} (13%)
υ_{72}		3282ms	3711	0.39	19.69	1.09	8.86	γ_{CH} (22%) + γ_{CH} (22%) + γ_{CH} (21%) + γ_{CH} (12%) + γ_{CH} (14%)
υ_{73}	3278w		3721	2.47	32.61	1.09	8.94	γ_{CH} (10%) + γ_{CH} (16%) + γ_{CH} (46%)
υ_{74}	3314w		3723	0.80	67.93	1.10	9.05	γ_{CH} (67%) + γ_{CH} (16%)
υ_{75}			3724	0.37	73.38	1.09	8.93	γ_{CH} (35%) + γ_{CH} (35%) + γ_{CH} (14%)
υ_{76}			3732	5.26	46.47	1.09	9.01	γ_{CH} (13%) + γ_{CH} (30%) + γ_{CH} (27%) + γ_{CH} (21%)
υ_{77}	3378w		3738	6.48	76.84	1.10	9.06	γ_{CH} (83%) + γ_{CH} (14%)
υ_{78}			3743	15.93	79.64	1.10	9.09	γ_{CH} (12%) + γ_{CH} (14%) + γ_{CH} (33%) + γ_{CH} (36%)
υ_{79}			3752	10.91	102.26	1.10	9.13	γ_{CH} (72%) + γ_{CH} (17%)
υ_{80}			3758	5.84	65.61	1.09	9.13	γ_{CH} (91%)
υ_{81}			3999	8.71	53.80	1.07	10.15	γ_{NH} (100%)

ν-stretching, δ-in-plane bending, Γ-out-of-plane bending, t-torsion , s-strong, m-medium, w-weak, ms-medium strong, vs-very strong.

NBO Analysis

NBO analysis gives the accurate possible natural Lewis structure picture of ø, because all orbital are mathematically chosen to include the highest possible percentage of the ED. Interaction between both filled and virtual orbital spaces information is correctly explained by the NBO analysis. It could enhance the analysis of intra- and inter- molecular interactions. The second order Fock matrix was carried out to evaluate donor (i) – acceptor (j) i.e. donor level bonds to acceptor level bonds interaction in the NBO analysis [24]. The result of interaction is a loss of occupancy from the concentration of electron NBO of the idealized Lewis structure into an empty non-Lewis orbital. For each donor (i) and acceptor (j), the stabilization energy E(2) associates with the delocalization i → j is estimated as:

$$E(2) = \Delta E_{ij} = q_i \frac{F(i,j)^2}{\varepsilon_j - \varepsilon_i}$$

Where q_i is the donor orbital occupancy, $\boldsymbol{\varepsilon}_j$ and $\boldsymbol{\varepsilon}_i$ are diagonal elements and F(i, j) is the off diagonal NBO Fock matrix element. NBO analysis provides an efficient method for studying intra- and inter-molecular bonding and interaction among bonds; and also provides a convenient basis for investigating charge transfer or conjugative interaction in molecular systems. Some electron donor orbital, acceptor orbital and the interacting stabilization energy resulted from the second-order micro disturbance theory are reported [25, 26].

The larger E(2) value the more intensive is the interaction between electron donors and acceptors i.e. the

more donation tendency from electron donors to electron acceptors and the greater the extent of conjugation of the whole system [27]. Delocalization of ED between occupied Lewis – type (bond or lone pair) NBOs and formally unoccupied (antibond or Rydeberg) non-Lewis NBOs corresponds to a stabilizing donor- acceptor interaction. NBO analysis has been performed on the N4MBA molecule at DFT/B3LYP/6-311G(d,p) level in order to elucidate, the intra-molecular hybridization and delocalization of ED within the molecule. The charge transfer within the molecule is more in $\pi \rightarrow \pi^*$ transition. This study reveals the energy transfer during inter-molecular interactions. Transition between πC1-C2 and π*C3-C4, π*C5-C6 bonds has the energy 56.02 and 30.05 kJ/mol respectively. Occupancy of π bands has lesser than σ bands which lead more delocalization. From the NBO study, we state that the atom having lone pair electrons transfer more energy to its acceptors. The E(2) values and types of the transition are shown in Table 3.

HOMO-LUMO Analysis

HOMO and LUMO are very important parameters for quantum chemistry. We can determine the way in which the molecule interacts with other species; hence, they are called the frontier orbitals. HOMO, which can be considered as the outermost orbital containing electrons, tends to give these electrons such as an electron donor. On the other hand; LUMO can be considered as the innermost orbital containing free places to accept electrons [28]. The HOMO and LUMO energy calculated by HF/6-311++G(d,p) and B3LYP/6-311G(d,p)/6-311++G(d,p) methods are shown in Table 4. This electronic transition absorption corresponds to the transition from the ground to the first excited state and is mainly described by an electron excitation from HOMO to LUMO. In the present study, the C=C, O-CH_3 and C-N bond have highest occupied MO and the LUMO prevails over the C-C bond in N4MBA. The atomic compositions of the frontier MO using B3LYP/6-311G(d,p) are shown in Fig. 4.

Table 3. Second order perturbation theory analysis of Fock matrix in NBO basis for N4MBA using B3LYP/6-311G(d,p)

Donor (i)	Type	ED/e	Acceptor (j)	Type	E(2)[a] (kJmol^{-1})	E(j)-E(i)[b] (a.u)	F(i,j)[c] (a.u)
C1-C2	σ	1.97	C1-C6	σ*	5.46	1.79	0.088
C1-C2	σ	1.99	C1-O11	σ*	0.81	1.62	0.032
C1-C2	σ	1.98	C2-C3	σ*	4.41	1.82	0.080
C1-C2	σ	1.97	C2-H7	σ*	1.63	1.65	0.046
C1-C2(2)	π	1.64	C1-C2	π*	0.72	0.79	0.017
C1-C2(2)	π	1.67	C3-C4	π*	56.02	0.50	0.150
C1-C2(2)	π	1.70	C5-C6	π*	30.05	0.50	0.111
C1-C6	σ	1.98	C5-H9	σ*	2.69	1.63	0.059
C1-C6	σ	1.98	C6-H10	σ*	1.56	1.63	0.045
C1-C6	σ	1.99	O11-C12	σ*	4.09	1.52	0.071
C1-O11	σ	1.97	C1-C2	σ*	1.03	2.03	0.041
C1-O11	σ	1.97	C1-C6	σ*	0.91	2.04	0.039
C1-O11	σ	1.98	C2-C3	σ*	1.14	2.07	0.043
C2-C3	σ	1.97	C3-C4	σ*	4.57	1.80	0.081
C2-C3	σ	1.98	C3-H8	σ*	1.44	1.66	0.044
C2-C3	σ	1.97	C4-C16	σ*	4.04	1.67	0.073
C2-H7	σ	1.99	C1-O11	σ*	0.91	1.39	0.032
C2-H7	σ	1.98	C2-C3	σ*	1.75	1.59	0.047
C2-H7	σ	1.97	C3-C4	σ*	4.14	1.58	0.072
C3-C4	σ	1.97	C4-C16	σ*	3.51	1.66	0.068
C3-C4	σ	1.98	C5-H9	σ*	2.87	1.62	0.061
C3-C4	σ	1.98	C16-H33	σ*	1.43	1.57	0.042
C3-H8	σ	1.97	C3-C4	σ*	1.46	1.57	0.039
C3-H8	σ	1.97	C4-C5	σ*	5.49	1.56	0.083
C4-C5	σ	1.94	C16-N17	σ*	1.44	1.89	0.047
C4-C16	σ	1.97	C5-C6	σ*	2.30	1.74	0.057
C4-C16	σ	1.98	N17-C18	σ*	5.35	1.60	0.082
C5-C6	σ	1.98	C6-H10	σ*	2.12	1.64	0.044
C5-C6(2)	π	1.64	C1-C2	π*	47.97	0.49	0.139
C5-C6(2)	π	1.67	C3-C4	π*	30.68	0.50	0.113
O11-C12	σ	1.97	C1-C6	σ*	3.23	1.94	0.071
C12-H14	σ	1.99	C1-O11	σ*	4.46	1.39	0.071
C6-N17	σ	1.98	N17-C18	σ*	2.42	1.90	0.061
C6-N17	σ	1.97	C18-C19	σ*	2.14	2.03	0.059
C16-N17(2)	π	1.65	C18-C20	π*	11.83	0.63	0.084
C18-C20(2)	σ	1.94	C16-N17	σ*	0.76	1.16	0.027
C19-C21(2)	π	1.66	C23-C25	π*	42.42	0.50	0.131
C21-C25	σ	1.98	O28-C29	σ*	1.12	1.53	0.037
C23-C25	σ	1.97	C18-C20	σ*	40.94	0.50	0.128
C29-H32	σ	1.98	O28-C29	σ*	0.53	1.30	0.023

[a]E(2) means energy of hyper conjugative interaction (stabilization energy)
[b]Energy difference between donor and acceptor i and j NBO orbitals.
[c]F(i,j) is the Fork matrix element between i and j NBO orbitals.

Table 4. HOMO LUMO energy calculated by HF and DFT methods

Parameter	HF/ 6-31G(d,p) (eV)	B3LYP/ 6-31G(d,p) (eV)	B3LYP/ 6-311G(d,p) (eV)
HOMO	-0.349	-0.305	-0.310
LUMO	-0.220	-0.206	-0.207
Energy gap (ΔE)	0.129	0.099	0.103

SCF energy = -658.4805 a.u.

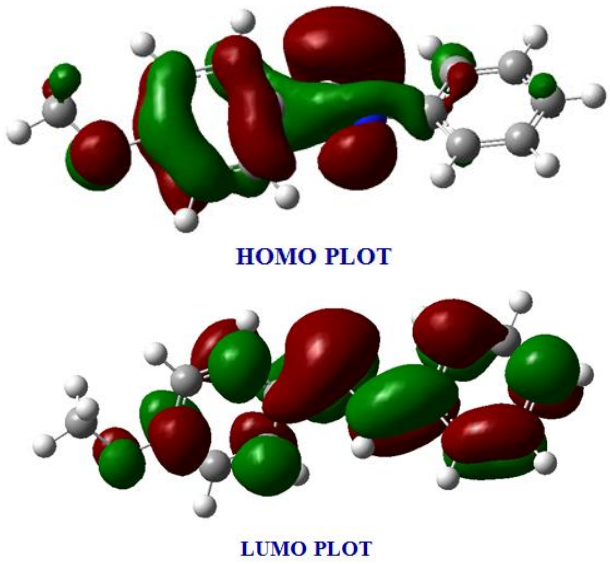

Figure 4. Molecular orbital surfaces for the HOMO and LUMO of the title compound computed at B3LYP/6-311++G(d,p) level

Other Molecular Properties

Mulliken Charges

The calculation of atomic charges plays an important role in the application of quantum mechanical calculations to molecular systems [29]. The charge distributions are calculated by Mulliken method [30] using HF/6-311++G(d,p), B3LYP/6-311G(d,p) and B3LYP/6-311++G(d,p) methods for the equilibrium geometry of N4MBA. The charge distribution on the molecule has an important influence on the vibrational spectra. The corresponding Milliken's plot is shown in Fig. 5. 5C possesses the most negative charge and 4C possesses the most positive charge by B3LYP/6-311++G(d,p) method.

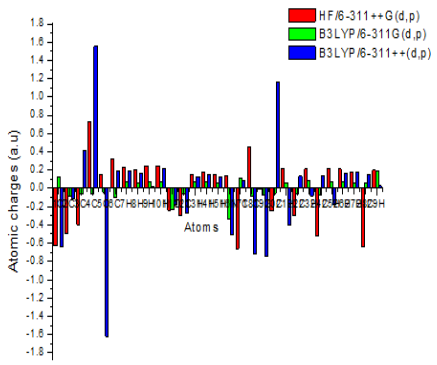

Figure 5. Comparison of different methods for calculated atomic charges of N4MBA

Thermodynamic Properties

The calculated thermodynamic parameters are presented in the Table 5. Scale factors have been recommended [31] for an accurate prediction in determining the zero-point vibrational energies and the entropy S. The variations in the zero-point vibrational energies seem to be insignificant. The total energies found to decrease with increase of the basis sets. The changes in the total entropy of N4MBA at room temperature at different basis sets are only marginal.

Table 5. Theoretically computed energies, zero-point vibrational energies, rotational constants, entropies and dipole moment for N4MBA

Parameters	HF/ 6-31G(d,p)	B3LYP/ 6-31G(d,p)	B3LYP/ 6-311G(d,p)
Total Energies (a.u)	-658.48	-665.74	-666.95
Zero point energy (kcal/mol)	170.59	157.41	157.41
Rotational constants (GHz)	2.46	1.02	1.11
	0.17	0.28	0.32
	0.16	0.24	0.26
Entropy (cal/mol/K)			
Total	114.93	116.50	116.49
Translational	41.94	41.94	41.94
Rotational	32.78	32.77	32.77
Vibrational	40.20	41.78	41.77
Dipole moment (D)	3.39	3.61	3.65

Conclusion

A complete vibrational and molecular structure analysis has been performed based on the quantum mechanical approach by *ab initio* HF and DFT (B3LYP) calculations. The computed and observed FT-IR and FT-Raman spectra are in close agreement with each other. NBO reflects the charge transfer within the molecule. HOMO and LUMO orbitals have been visualized. Moreover, several thermodynamic properties and Mulliken charges are also calculated.

References

[1] S.Kumar, D.G.Ladha, P.C.Jha and N.K.Shah "Theoretical study of Chloro-N-4-(methoxybenzylidine)aniline derivatives as corrosion inhibitors for zinc in hydrochloric acid", International Journal of Corrosion, (2013) 1.

[2] K.Srinivasan, R.Birvaganesh, R.Gandhimathi, P.Ramasamy, J.Cryst. Growth, 236 (2002) 381.

[3] A.N.Azariah, A.S.H.Hameed, T.Thenappan, M.Noel, G.Ravi, Mater. Chem. Phys., 8 (2002) 90.

[4] J. Deli, T. Lorand, D. Szabo, A. Foldesi, Potentially bioactive pyrimidine derivatives. 1. 2-Amino-4-aryl-8-arylidene-3,4,5,6,7,8-hexahydroquinazoline, Pharmazie 39 (1984) 539.

[5] G.K. Kaushal, Synthesis and characterization of photo-cross-linkable main- chain liquid-crystalline polymers containing bis benzylidine cycloalkanone units, Polymer 36 (1995) 1903.

[6] M. Ogawa, Y. Ishii, T. Nakno, S. Irifune, Jpn. Kohai Tokyo. Chem. Abstr. 63 (1988) 238034.

[7] V.Balachandran, G.Santhi, V.Karpagam, A.Lakshmi, DFT computation spectroscopic studies of N-(p-methoxybenzylidine)aniline, a potentially useful NLO material, Journal of Molecular Structure, 1047 (2013) 249.

[8] Akira Takase, Sakumitsu Sakagami, Kazuhiro Nonaka and Toshiaki Koga, Spectroscopic studies of the thermochromism of N-(2-hydroxy-4-methoxybenzylidine)-4- nitroaniline,

Journal of Raman Spectroscopy, 24(7) (1993) 447.
[9] J.W.Lewis and C.Sandorfy, An infrared study of the photoisomerization of N-benzylidineaniline, Canadian Journal of Chemistry, 60 (2013) 1720.
[10] Helmi Neuvonen, Kari Neuvonen and Ferenc Fulop, Substituent cross-interaction effects on the electronic character of the C-N bridging group in substituted benzylidine anilines – Models of molecular cores of mesogenic compounds. A ^{13}C NMR study and comparison with theoretical results.
[11] Gaussian 03W program, (Gaussian Inc. Walling ford CT) (2004).
[12] H.B. Schlegel, Optimization of equilibrium geometries and transition structures, J. Comput. Chem. 3 (1982) 214.
[13] P. Pulay, G. Fogarasi, G. Pongor, J.E. Boggs, A.Vargha, Combination of Theoretical *ab initio* and Experimental Information to Obtain Reliable Harmonic Force Constants. Scaled Quantum Mechanical Force Fields for Glyoxal, Acrolein, Butadiene, Formaldehyde, and Ethylene, J. Am. Chem. Soc. 105 (1983) 7037.
[14] A.P. Scott, L. Radom, Harmonic Vibrational Frequencies: An Evaluation of Hartree-Fock, Møller-Plesset, Quadratic Configuration Interaction, Density Functional Theory, and Semiempirical Scale Factors, J. Phys. Chem. 100 (1996) 16502.
[15] Isa Sidir, Yadigar Gulseven Sidir, Mustafa Kumalar, Erol Tasal, *Ab initio* Hartree-Fock and density functional theory investigations on the conformational stability, molecular structure and vibrational spectra of 7-acetoxy-6-(2,3-dibromopropyl)-4,8-dimethylcoumarin molecule, J. Mol. Struct. 964 (2010) 134.
[16] D.L. Pavia, G.M. Lampman, G.S. Kriz, Physics Editor: J. Vondeling, Introduction to Spectroscopy: A guide for student of organic chemistry, Third Edition, Thomson Learning, (2001), p.579.
[17] Y.R.Sharma, Elementary Organic Spectroscopy, Principles and Applications, S.Chand Publications, New Delhi, (2010).
[18] T. Shimanouchi, Y. Kakiuti, I. Gamo, out-of-plane CH Vibrations of Benzene Derivatives, J. Chem. Phys, 25 (1956) 1245.
[19] N.P. Sing, R.A. Yadav, Vibrational studies of trifluoromethyl benzene derivatives I: 2- amino-5-chloro and 2- amino-5-bromo benzotrifluorides, Ind. J. Phys. B 75 (2001) 347.
[20] V. Krishnakumar, R. John Xavier, Density functional theory calculations and vibrational spectra of 3,5-dibromopyridine and 3,5-dichloro-2,4,6-trifluoropyridine, Spectrochim. Acta 61A (2005) 253.
[21] D.A. Prystupa, A. Anderson, B.H. Torrie, Raman and infrared study of solid benzyl alcohol, J. Raman Spectrosc. 25 (1994) 175.
[22] R.K. Yadav, N.P. Singh, R.A. Yadav, Vibrational studies of trifluoromethyl benzene derivatives II: 5-amino-2-fluoro and 5-amino-2-chloro benzotrifluorides, Ind. J. Phys. B 77 (2003) 419.
[23] D.N. Sathyanarayana, Vibrational Spectroscopy, Theory and Applications, New Age International Publishers, New Delhi, (2004).
[24] M. Szafran, A. Komasa, E.B. Adamska, Crystal and molecular structure of 4-carboxypiperidinium chloride (4-piperidinecarboxylic acid hydrochloride, J. Mol. Struct. 827 (2007) 101.
[25] C. James, A. Amal Raj, R. Rehunathan, V.S. Jayakumar, I.H. Joe, Structural conformation and vibrational spectroscopic studies of 2,6-bis(p-N,N-dimethyl benzylidine) cyclohexanone using density functional theory, J. Raman Spectrosc. 37 (2006)1381.
[26] L. Jun-na, C. Zhi-rang, Y. Shen-fang, J. Zhejiag, Study on the prediction of visible absorption maxima of azobenzene compounds, Univ. Sci. 6B (2005) 584.
[27] S. Sebastian, N. Sundaraganesan, The spectroscopic (FT-IR, FT-IR gas phase, FT-Raman and UV) and NBO analysis of 4-Hydroxypiperidine by density functional method, Spectrochim. Acta 75A (2010) 941.
[28] G. Gece, The use of quantum chemical methods in Corrosion inhibitor studies, Corros. Sci. 50 (2008) 2981.
[29] S. Gunasekaran, S. Kumaresan, R. Arunbalaji, G. Anand, S. Srinivasan, Experimental and theoretical investigations of spectroscopic properties of N-acetyl-5-methoxytryptamine, J. Chem. Sci. 120 (2008) 315.
[30] R.S. Mulliken, Electronic Population Analysis on LCAO-MO Molecular Wave Functions, J. Chem. Phys. 23 (1955) 1833.
[31] M.A. Palafox . Scaling factors for the prediction of vibrational spectra. I. Benzene molecule, Int. J. Quantum. Chem. 77 (2000) 6.